HapTag: A Compact Actuator for Rendering Push-Button Tactility on Soft Surfaces

Yanjun Chen
Institute of Software, Chinese Academy of Sciences
Beijing, China
chenyanjun@iscas.ac.cn

Xuewei Liang*
Xi'an jiaotong university
Xi'an, China
liangxuewei2017@stu.xjtu.edu.cn

Si Chen*
Stony Brook University
Stony Brook, United States
Si.Chen.2@stonybrook.edu

Yuwen Chen†
Institute of Software, Chinese Academy of Sciences
Beijing, China
chenyuwen20@mails.ucas.ac.cn

Hongnan Lin
Georgia Institute of Technology
Atlanta, United States
hlin324@gatech.edu

Hechuan Zhang†
Institute of Software, Chinese Academy of Sciences
Beijing, China
zhanghechuan21@mails.ucas.ac.cn

Chutian Jiang
Institute of Software, Chinese Academy of Sciences
Beijing, China
cdswjct@gmail.com

Feng Tian†
Institute of Software, Chinese Academy of Sciences
Beijing, China
tianfeng@iscas.ac.cn

Yu Zhang
Xi'an Jiaotong University
Xi'an, China
zhang.yu@xjtu.edu.cn

Shanshan Yao
Stony Brook University
Stony Brook, United States
shanshan.yao@stonybrook.edu

Teng Han‡
Institute of Software, Chinese Academy of Sciences
Beijing, China
hanteng@iscas.ac.cn

Figure 1: HapTag is a compact haptic actuator that can be attached or integrated into surfaces, to provide haptic sensations for everyday touch interactions. (a) The effect of HapTag being activated; (b) HapTag embedded in the sleeve is activated when the user pinches; (c) Using HapTag as an interactive watchband.

ABSTRACT

As touch interactions become ubiquitous in the field of human computer interactions, it is critical to enrich haptic feedback to improve efficiency, accuracy, and immersive experiences. This paper presents HapTag, a thin and flexible actuator to support the integration of push button tactile renderings to daily soft surfaces. Specifically, HapTag works under the principle of hydraulically amplified electroactive actuator (HASEL) while being optimized by

*Both authors contributed equally to the paper
†Yuwen Chen and Hechuan Zhang are also with School of Computer Science and Technology, University of Chinese Academy of Sciences. Feng Tian is also with College of Artificial Intelligence, University of Chinese Academy of Sciences.
‡Corresponding author.

UIST '22, October 29-November 2, 2022, Bend, OR, USA

ACM ISBN 978-1-4503-9320-1/22/10…$15.00
https://doi.org/10.1145/3526113.3545644

embedding a pressure sensing layer, and being activated with a dedicated voltage appliance in response to users' input actions, resulting in fast response time, controllable and expressive push-button tactile rendering capabilities. HapTag is in a compact formfactor and can be attached, integrated, or embedded on various soft surfaces like cloth, leather, and rubber. Three common push button tactile patterns were adopted and implemented with HapTag. We validated the feasibility and expressiveness of HapTag by demonstrating a series of innovative applications under different circumstances.

CCS CONCEPTS

• **Human-centered computing → Haptic devices**.

KEYWORDS

Haptic, force feedback, flexible actuator, dielectric material

ACM Reference Format:

Yanjun Chen, Xuewei Liang, Si Chen, Yuwen Chen, Hongnan Lin, Hechuan Zhang, Chutian Jiang, Feng Tian, Yu Zhang, Shanshan Yao, and Teng Han. 2022. HapTag: A Compact Actuator for Rendering Push-Button Tactility on Soft Surfaces. In *The 35th Annual ACM Symposium on User Interface Software and Technology (UIST '22), October 29-November 2, 2022, Bend, OR, USA*. ACM, New York, NY, USA, 11 pages. https://doi.org/10.1145/3526113.3545644

1 INTRODUCTION

The development of Internet of Things (IoT) leans towards outfitting physical environments with digital abilities and experiences, e.g., integrating sensing components to ordinary, familiar objects like clothing and articles for daily use, which as a result, afford a variety of touch and gesture interactions [23, 33, 44, 53, 54]. For instance, users can skip a song by swiping their sleeve, and take a picture by tapping on a shoulder strap [30]. These novel interfaces usually involve actions that imitate physical world interactions with input methods like buttons and other control components. A clear benefit is users are already familiar with those UI components, e.g., pressing a button to switch on/off light. However, few considerations have been given to implementations used to communicate helpful visual, auditory, or haptic feedback in the interactions. It feels very different when pressing a button on the keyboard, and pressing a button on the sleeve.

Push buttons are essential UI elements and we are used to seeing them in our day-to-day life, but there arises a challenge to convey haptic sensations of a push button on soft and flexible surfaces like clothes. A push button is a common yet simple mechanism to transduce user actions like pressing, slapping, clicking, and pinching, utilized in mechanical and electronic devices. Push buttons are made with various mechanisms, such as springs, rubber, and metal domes, for producing highly distinguishable tactile responses, or tactility. However, they typically consist of rigid components and are hard to adapt to soft interfaces. This has motivated the development of more compact, lightweight, soft, and even elastic actuators [8, 25, 28, 29, 41, 49]. A majority of the work utilizes electroactive polymer actuators (e.g., dielectric elastomer actuators, known as DEA), which realize high-speed vibrotactile actuating but suffer from insufficient altering. Others use pneumatic drivers (e.g., pneumatic artificial muscle, known as PAM), which achieve large deformation and high actuation stress, but require auxiliary pumps [2].

This paper presents HapTag, a thin and flexible actuator to support haptic rendering of push buttons on soft surfaces. HapTag is in a compact form, 15 mm in width/length, 0.6 mm in height and 350 mg in weight. It can be attached on top of, inside of, or underneath various soft surfaces and provide configurable button-like tactile feedback when a user presses on or squeezes with the surfaces. HapTag is built upon the hydraulically amplified electroactive actuator (HASEL), a recently emerging variant of DEA, which combines the speed and versatility advantages of electroactive and pneumatic methods [43]. We further investigate the actuation performance with various dielectric materials (e.g., PVDF and TPU), and structure design with an integrated pressure sensing unit, resulting in a self-contained sensing-actuating mechanism that can deliver desirable haptic feedback. Compared with previous work in building soft vibrotactile patches [8, 49], HapTag has distinctive qualities in rendering responsive force and displacement, maximally outputting 259 mN and 525 μm at the voltage of 5 kV, respectively. This allows HapTag to display push button tactility by recreating rapid changes in reaction force.

We modulated the contact force using 3 different patterns and validated the haptic rendering capabilities under a set of circumstances, where users were asked to press, pinch, or mid-air click with soft surfaces made of fabrics or polymers. The patterns were designed to make impressive and distinguishable push button tactile responses. Results show that these haptic profiles are clearly rendered and distinguishable. As suggested by the results, the mean accuracy of recognizing the type of button in each combination of independent variables (the tactile responses, the surface materials, and the interaction gestures) are relatively similar and each accuracy level is higher than 90%. The response time for recognizing the type of button in each combination is short. For instance, the average response time of the three tactile responses is around 600 ms. For instance: Linear Button (546 ms), Clicky Button (698 ms), and Self-Lock Button (640 ms).

The paper presents the following contributions: i) the design and implementation of HapTag as a compact actuator to deliver configurable and clear push button tactile responses; ii) validation of 3 push button tactility with 3 use methods on 2 types of soft surfaces.

2 RELATED WORK

HapTag is designed as an attachable or integratable module to provide precise push button tactile feedback on soft surfaces. It extends previous work on surface haptics, as well as contributes to the category of soft and compact actuators.

2.1 Surface Haptics

Surface haptics refers to the application of variable forces on a user's finger as it interacts with a surface such as a touchscreen [4]. This line of research got popular with the widespread use of touchscreens on mobile phones, tablets, tabletops, and interactive displays. A majority of the work explored electromagnetic actuators that create vibrotactile feedback in either normal or tangential directions. Vibration motors such as linear actuators are commonly equipped in mobile and wearable devices, and have been used to play short vibration pulses and mimic a home button press, relay system notifications, and reinforce audio alerts [12]. In recent work, vibrotactile feedback has been shown promising in presenting compelling effects and improving player experiences on mobile phones [36]. Besides, vibrotactile feedback is capable to convey emotion and affect [32, 48]. Using multiple actuators simultaneously or in sequence can create distributed surface haptics because of the existence of perception illusion [3, 27]. It is also possible to create lateral vibrations to let users feel as if there is a relative displacement between finger and surface, which can even render virtual texture [45]. Researchers have devised ways to modulate the friction felt by finger sliding on the surface. For instance, the friction can be decreased by using actuators that generate ultrasonic waves due to active lubrication [22, 46], and increased by using electrostatic actuation that generates electrostatic attractive forces [5, 9, 39].

Besides vibrotactile sensations, other tactile surfaces have been explored using dedicated materials and mechanisms. Smart fluids such as magnetorheological fluids act as a mechanism that reacts to an external magnetic or electric field and changes the evident stiffness [13, 47]. Alternative solutions are investigated including particle jamming [6] to change the stiffness of touch surfaces. Shape-changing display represents another category of mechanism to enable physical visualization and tactical exploration. Their essential affordance of haptic interactions on active surfaces has been exploited to enrich applications in virtual and augmented reality domains [7, 37].

With the increasing interest in turning everyday interfaces into interactive ones, there emerge several works that retrofit existing surfaces with haptic feedback [10, 35]. A recent work is HapSense [49], in which the authors develop an electroactive polymer based actuator to provide embedded vibrotactile feedback. MagnetIO [18] takes an alternative approach and deployed a voice coil on finger and stretchable magnetic patches on objects to create vibrotactile haptics. Though promising, the proposed devices face confounding challenges on limited force output, being restricted in providing a short burst of force output. For instance, HapSense [49] is reportedly capable of generating an output force of $6.7mN$ and displacement of $4.1\mu m$ at an input voltage of $300V$.

HapTag takes a different technical approach to tackle the limitation. It is built upon the emerging HASEL technique and customized in material and structure design, resulting in distinctive qualities in haptic force rendering and displacement output.

2.2 Compact and Soft Actuators

The development of embedded/integrated haptic interfaces and on-skin tactile devices has activated the need for soft and compact actuators. According to the previous research, soft actuators can be roughly divided into two categories in terms of actuation methods: one is directly activated by an external force, such as pneumatic and electromagnetic actuators [15, 38]; the other uses the nature of the material itself, through external stimuli, such as light, electricity, etc., causing the material itself to deform, e.g. electroactive actuators [20].

External force actuators have been investigated over a relatively long period, and some types have already formed mature commercial products. For example, voice coil motors have been widely used in scenarios that provide tactile sensation through vibration [51]. Another distinct advantage of this type is its ability to deliver larger forces. For example, pneumatic actuators, which are similar to hydraulic actuators in the actuation principle, can output a constant and steady force, and the amount of force can be adjusted by regulating the input gas supply [11]. However, in the field of soft actuators, external force type presents an unignorable disadvantage, namely the great difficulty in miniaturization and softening. In the process of integration, the size of external force suppliers, such as air pumps, etc., is hard to modify. Likewise, the actuators that utilize electromagnetic induction, e.g. voice coil motors, cannot be realized in principle by using all soft materials because of the requirement of electromagnetic components.

To realize more compact and softer actuators, material-type actuators that are activated by the material itself undergoing deformation by stimulation are gaining attention [18]. The representative of this type of actuator is the electroactive actuator. Electroactive actuators can be subdivided into electronic and ionic ones. Although the principles are slightly different, they are generally due to material deformation caused by uneven charge or particle distribution when a voltage is applied to the material [42, 52]. Compared to the external force-type actuators, the material-type actuators can achieve a purely flexible material composition [50]. As no rigid material is required to provide actuation support, this type of actuator presents a significant superiority in terms of lightweight and flexibility. By using highly biocompatible materials, such as silicone, material-based actuators hold great promise for applications in the field of wearable devices [20]. However, these characteristics also have a negative impact on such actuators, i.e., the lack of ability to generate high actuation force.

Combining these two types of actuators, the question of how to achieve a compact structure, a soft and thin device, and wearability while being able to provide sufficient actuation force is a key research topic in the field of soft actuators.

3 DESIGN AND IMPLEMENTATION OF HAPTAG

In this work, we intended to make a thin and compact actuator that can be attached to ambient surfaces and provide a strong force and displacement correlation for rendering push button tactility. To obtain the two key properties, we designed HapTag based on the fundamental concept of HASEL actuator, an emerging mechanism of soft electronic actuators. We made design improvements regarding the material to advance its thinness and structure to strengthen the force-displacement correlation.

3.1 Operation Principle and Design

It is a type of electroactive actuator, which achieves the zipper effect by applying a voltage that causes charges to gather on both sides of the dielectric layer to produce an electrostatic force.

The force is theoretically derived from the Maxwell stress which is based on the following equation:

$$P = \varepsilon \frac{U^2}{2d^2} \tag{1}$$

Where ε is the dielectric constant, U is the applied voltage and d is the distance between top and bottom electrode.

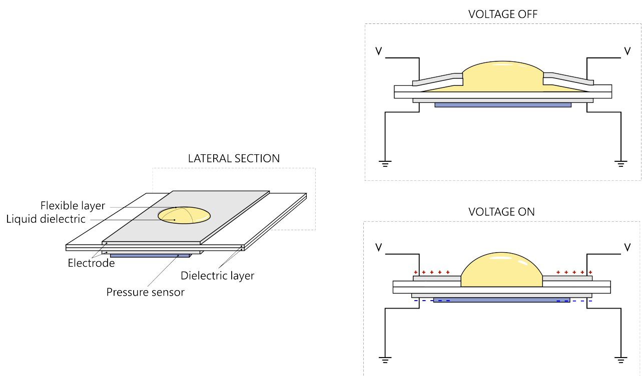

Figure 2: Schematic diagram and Actuation principle of HapTag.

A schematic diagram of the driving principle of HapTag is shown in Figure 2. When no voltage is applied, the injected dielectric fluid fills the gap between the upper and lower dielectric layers, making them static at a certain angle. When voltage is on, electrostatic pressure is generated. Since the distance between the two electrodes is minimal at the sealing edge, from here the dielectric liquid starts to be squeezed and transferred. As presented in Figure 2 Voltage on a diagram, along with this tendency of movement, the dielectric fluid is gradually squeezed to the center where the electrode material is not attached. This is called the zipping effect which is used to amplify the electrostatic pressure.

Due to the dielectric liquid volume conversion, the filling of more liquid at the center is elastic deformation of the upper layer material, resulting in an out-of-plane displacement and output force in the vertical direction. The force depends on

$$F = \pi r^2 \cdot P \tag{2}$$

where r is the radius of the central part, and P is the electrostatic pressure.

In the currently available studies, when the actuation force is used as the prominent performance parameter, the size of the device is usually large and difficult to be applied in interactive interfaces. The HASEL structure, which this paper is inspired by, makes improvements in size and flexibility. As mentioned above, there is a strong enthusiasm for research on soft actuators based on the principal technique of HASEL. Several derivatives of HASEL have been employed to create haptic feedback on human skin [50]. However, there are still many problems with the previous research results. First, the low actuation force and the small displacement are noteworthy. Besides, the driving force it generates is still not a very substantial value [16]. Second, current research with HASEL actuators is mainly focused on exploring the properties of the material, etc., while its potential applications have not been fully exploited.

In this paper, we focused on the application scenario of the haptic interaction interface and explored the application potential of HASEL-based actuators in daily life. Based on such a working principle, HapTag made targeted design improvements according to the interaction needs of the application scenario. As shown in Figure 2, HapTag was constructed using a sandwich structure (flexible layer, upper layer, and lower layer), based on HASEL technique. Here we have improved the dielectric layer material and the flexible layer material. In applications of haptic interactions, the force and displacement correlation that the actuator can provide is a critical factor. Commonly used dielectric layer materials include Polydimethylsiloxane (PDMS), Ecoflex, Thermoplastic polyurethane (TPU), Polyvinylidene fluoride (PVDF), etc. After experimental validation, TPU was chosen as dielectric elastomer layers due to its mechanical and dielectric properties for the relative permittivity, its thermoplasticity enables a significantly simplified process to form liquid chambers with hot pressing, and low cost of fewer than $\$4/m^2$. In addition, TPU as a dielectric layer can achieve the apparent zipping effect with a high liquid volume conversion rate. PDMS was chosen as the flexible layer material, as PDMS has a moderate modulus of elasticity, appropriate for force transmission.

In summary, this paper explores alternative derivatization of HASEL actuator with stronger force and displacement rendering capability, yet with a simpler fabrication process, and is the first to discuss such types of actuators' advantages in establishing haptic tags to support touch interactions on everyday displays scenarios among all the current human computer interaction research.

3.2 Fabrication

HapTag was composed of double dielectric elastomer layers coupled to compliant Polyethylene terephthalate (PET) metalized film. The chamber sealed by these two films was filled with dielectric liquid as a motion amplifier. An inner stretchable film was bonded on top to direct contact with the skin. To further enhance the film stretchability for design requirements, we tested the performance of the cover layer made from mixtures of PDMS and Ecoflex 00-30 (Smooth-On, Inc.) at various ratios, with displacement and force as a function of fluid pressures for these films. The results were shown in Figure 3, the cover layer exerted gradually escalated out-of-plane displacements with rising percentages of Ecoflex. Higher percentages weakened force feedback and complicated fabrication.

The detailed fabrication process was illustrated in Figure 4. The fabrication process was separated into four steps: (1) the cover layer, (2) the upper layer, (3) the lower layer, and (4) the integration of all of the above three parts and a force sensor to construct HapTag. Detailed fabrication processes were listed below, with the necessity and relevance of those treatments, and experimental validation of chosen materials.

(1) The cover layer was first fabricated through spin-coating a PDMS: Ecoflex 00-30 film (weight ratio 1: 1, 50 μm of thickness) followed in a solidified form by the laboratory oven (75°C, 60 min).

(2) For the fabrication of the upper layer, a PET membrane metalized with patterned aluminum (50 μm) was first exposed to an O_2 plasma for 60 seconds in a plasma cleaner (PDC-MG) for a minute at 100 W to activate the surface. The side of the electrode-patterned surface of the membrane was easily bonded with TPU (100 μm of

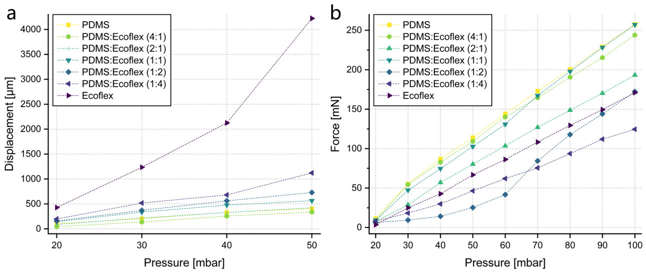

Figure 3: Measurement of displacement and force for films with different ratios of PDMS and Ecoflex 00-30 mixed. (a) Measured displacement as a function of pressure from 20 to 50 mabr; (b) Measured force versus pressure from 20 to 100 mabr.

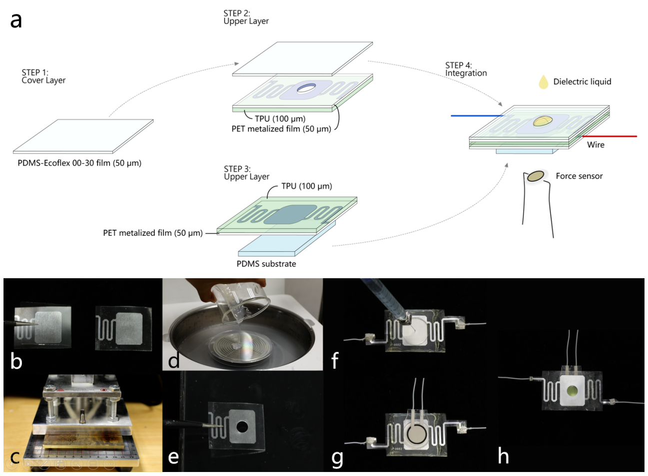

Figure 4: HapTag production process and display. (a) The specific steps of HapTag Fabrication; (b) Comparison of before and after hot pressing; (c) Hot pressing machines; (d) The PDMS and Ecoflex 00-30 solution was poured onto the substrate in the spin coaster; (e) Bonding the cover lay; (f) Dielectric fluid was injected into HapTag; (g) Adhesion of force sensors; (h) HapTag.

thickness) by the hot pressing process (170 $^{\circ}C$). The membrane was immersed in 5% (3-Aminopropyl) trimethoxysilane (APTMS, 97%) solution for 30 *mins* at 50 $^{\circ}C$ for surface treatment, to enhance the strength of the bonding between TPU and PDMS [40]. Then, after being dried and cleaned, a hole of 7 *mm* diameter was punched in the middle of this upper layer. To bond the cover layer, the side of the electrode-free surface of the membrane was once more exposed to O_2 plasma for surface treatment.

(3) The process of bonding the TPU to the PET metalized film structure was similar to those of the upper layer. Additionally, to prevent liquid leakage, the PDMS substrate was bonded to the bottom of the PET layer. Compression around the needle could form a fluid-free seal after filling the fluid with a thin needle.

(4) The upper layer with the cover layer and the lower layer was also bonded by hot pressing to form the structure of the shell. This sealing area was square with an inner diameter of 14 *mm*, slightly smaller than the area of the electrodes. The bio-based natural ester dielectric liquid (Envirotemp FR3) was injected through the PDMS substrate of the lower layer. In order to connect the external circuit, silver nano paste as a wire-to-electrode adhesive was applied to the upper and lower electrodes respectively, before having been solidified in a laboratory oven (60$^{\circ}C$, 120*mins*). A force sensor (FlexiForce A201-1) was placed at the bottom of the PDMS substrate using ultra-thin 3M467MP double-faced adhesive tape, to detect whether the simulated button was triggered by the user.

The fabrication process is highly reproducible and scalable. Following the above four steps, actuators can be manufactured repeatedly with small variances. This ensures the stability of the device during use. At the same time, the equipment used for fabrication here is commercially available and requires a low level of operator involvement, thus minimizing the errors introduced by the experimental operations. In addition, most of the production steps are performed by the heat press. The hot pressing technology is a mature and stable process that is easy to produce in mass production, which makes HapTag highly applicable and has a high commercial potential.

3.3 Actuation

HapTag prototype consisted of a high voltage power supply and a force sensor. The actuator was driven using a high voltage power supply programmed by Arduino to generate user-controllable voltages up to 5 kV. The high voltage power was provided by DC/DC converter (A50P-5 XP Power) and high voltage switch, which enabled square signals up to 1 kHz. The voltage was controlled by two optocouplers (OC100G), as illustrated in Figure 5. The DC/DC converter and optocouplers could be both controlled by Python HVPS user interface [34], parameters of which can be changed precisely, including voltage and high-frequency switching.

Specifically, the level of the voltage applied determined the volume of the fluid pushed into the stretchable center, which formed a raised bump with certain displacement and feedback force. The activation of the high-frequency switching can rapidly neutralize the voltage of the upper and lower electrodes, thereby forming a rapid depression haptic feeling due to the removal of the force. These parameters can be used to design haptic patterns, i.e. the timing, occasion, level, and duration of the tactile feedback generated. For safety purposes, the amplitude of output current was limited strictly. Additionally, the PET film separating the electrodes had reliable insulating property. In the latest work, Mitchell et al. presented a pocket-sized high voltage power supply [19], which offered a way of miniaturization and multiplication.

The force sensing thin-film resistor (FlexiForce) was used to detect the degree of finger pressing and pinching, which maintained a range of 0.4N and reached the linearity of +/-3%. Such a sensor was particularly designed for detecting the activation signal (whether the simulated button was being pushed by users) of the tactile response.

3.4 In-Lab Measurement

Based on the performance requirements of the design, the tests focused on measuring both displacement and force. For displacement

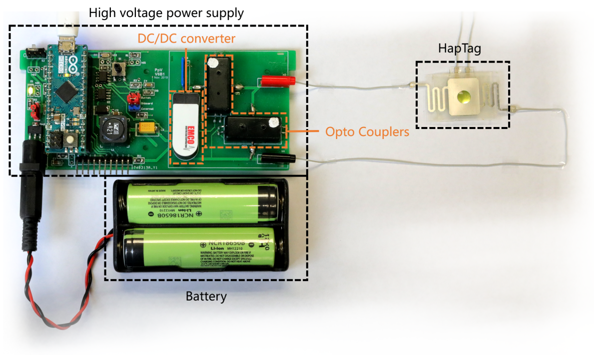

Figure 5: The overall HapTag system.

measurements, we used Keyence IL-S025, a linear position sensor with 1 μm repeatability. The sensor was mounted vertically above HapTag (Figure 6a). For force measurements, a Quartz force sensor (KISTLER Type 9207) with high sensitivity for measuring dynamic compressive forces in the range of less than 1 mN was placed on a vertically motorized platform, adjusting the height of the force sensor for adequate contact with HapTag film (Figure 6b). Each measurement was repeated 10 times under different voltages, from 0 kV to 5 kV with an increasing step of 0.5 kV. The measurements were then averaged over the maximum displacement and force as the final data.

As shown in Figure 6c&d, HapTag has maximum displacement and vertical force under 5 kV up to 525 μm and 259 mN respectively. The rapidly increasing displacement figure indicates that zipping occurred between 0.5 kV and 2 kV, while the slope of the displacement gradually decreases with the subsequent higher voltages applied owning to the limited flexibility of the PDMS-Ecoflex films. The electrical breakdown is observed for 50 μm PDMS-Ecoflex films at voltages higher than 5 kV, which is the reason that the measurement no longer continued under higher voltage. No significant effect was found in measurements of the displacement and force when the actuator was placed flat, vertically, and upside down, which might be attributed to the elastic dielectric layer restricting the flow of the liquid with the high viscosity. Throughout all tests, HapTag is able to produce stable out-of-plane displacement and force, which is quite acceptable compared with the results of HAXEL technique maintaining a maximum performance of 0.5 mm displacement and 300 mN force [16].

The performance under different loads was tested to illustrate force feedback rendering ability of HapTag. Five loads with the same contact area but different weights (10 g, 20 g, 30 g, 40 g, 50 g) were placed on HapTag surface, respectively, and the resulting displacements were recorded by the linear position sensor. The driving voltage of the whole experiment was 5 kV, with a 1 Hz switching frequency. The results indicate that HapTag is able to sustain weights heavier than itself (350 mg) and produces the desired displacement, as illustrated in Figure 7. Compared to the unloaded case, a significant reduction in recovery time is observed in the loaded case, especially at 30 g, where the actuator took 70 ms to go from 10% to 90% of the full stroke and 82 ms to return from 90% to 10%.

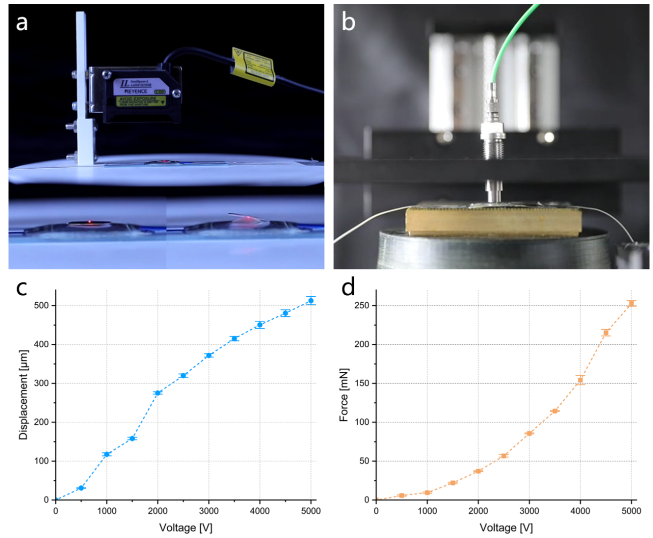

Figure 6: Testing process and results. (a) Displacement measurement instruments; (b) Force measurement instruments; (c) Measured displacement as a function of voltage; (d) Measured force versus Voltage.

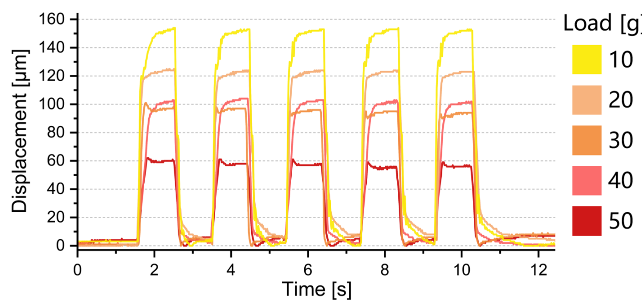

Figure 7: Measured displacement as a function of time for different load.

HapTag weighing 250 g (the main actuation components) produced a maximum of 40.38 μJ, for an energy consumption of 0.16 J/kg and a power density of 2.31 W/kg. Additionally, the power consumption was 186 mAh under 5 kV driven voltage. The maximum power of rendering increased due to the escalated voltage, ranging from 0.714 W at 3 kV to 1.482 W at 5 kV in an essentially linear fashion. Theoretically, the batteries with 6800 mAh capacity can run up to 36 hours, with haptic rendering 19303 times. These features verified the competence of HapTag to render haptic while users pressed.

4 TACTILE RESPONSES OF HAPTAG

HapTag aims to enrich haptic feedback of push button based interactions on daily soft surfaces. We designed tactility profiles based on 3 classic types of push buttons, and validated the implementation via measuring their force-displacement curves.

4.1 Haptic Profiles

Different from previous approaches that haptically generate button-click feedback with vibrotactile sensations [26], HapTag delivers tactile responses with actual force and displacement (FD) output. Based on haptic modeling theories for physical push buttons [17, 21, 24, 31], a critical factor that affects the haptic perception is the force-displacement model, which is the relationship between output force and out-of-plane displacement based on measurements. The implementation of HapTag utilized electric input and provided fast responses, resulting in configurable mappings between output force and displacement. Therefore, we took this conventional FD-model approach and used 3 classic push-button tactile profiles to characterize our design.

Here we composed 3 force-displacement profiles with HapTag with distinct characteristics to produce different haptic sensational feedback upon a user's click or press action (Figure 8). Specifically. Profile A is designed to simulate a linear button, with smooth force and displacement curves, with no tactile landmarks during both press and release processes. These types of buttons provide a sense of pressing a spring [24]. Profile B produces more changes during press-down and a stronger sense of "bump", like "clicky" buttons that are commonly seen on keyboards. Profile C conveys the process of a self-lock button, where the sense of bumps is produced in both the press and release processes. The operation method used to control the output and generate desired tactile responses was detailed in the Actuation section. It is worth noting that we did not intend to reproduce the exact haptic sensations of the physical buttons, which was way more complex. Instead, the imitation of the FD models provided initial insights for various haptic patterns that could be rendered by HapTag to produce push-button like tactile feedback with its structure.

4.2 Force-Displacement Measurement

Force displacement curve measurement was undertaken on a vertically motorized platform in which the force sensor and the displacement sensor as described were vertically shifted. The slip platform underwent a uniform downward motion at 0.15 mm/s to simulate the pressing behavior, and a uniform upward motion at the same velocity to simulate the releasing behavior. The motion details were recorded by the force sensor and displacement sensor continuously as the vertically motorized platform moved. The results of the measurement were shown in Figure8. It can be seen that HapTag followed clear FD patterns that are distinguishable, and reflected the attributes of the force-displacement curves for the desired push-button tactile feedback.

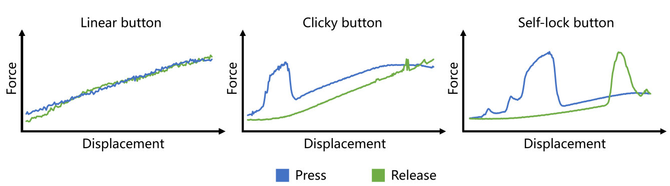

Figure 8: Three haptic profiles were composed to provide different sensations of buttons.

5 USER STUDY: PERCEPTION OF THE TACTILE RESPONSES

We validated the performance of HapTag and how well users can perceive and distinguish the tactile responses in simulated using scenarios, including where and how it will be used. Specifically, we sought to understand the effects of *tactile responses*, *surface materials*, and *interaction gestures* on the recognition of different haptic feedback formed by HapTag.

5.1 Experimental Design

Our study contained three independent variables (IVs): *tactile responses*, *integration materials*, and *interaction gestures*. The three interaction gestures (i.e., touch, pinch, in-air) were chosen considering where and how the actuator could be applied. It can be attached on top of or embedded inside of various flexible surfaces for interaction with touch/press or pinch gestures. Some examples are illustrated in Figure 1 & 13. Pinch meant using the thumb and index finger to 'squeeze' from both sides of the surfaces (Figure 9b). In-air click was considered for the use of wearable devices in VR/AR (Figure 9c). In addition to tactile responses (i.e., the linear button, the clicky button, and the self-lock button), we included surface materials as an IV because HapTag was supposed to be deployed on different types of soft surfaces. Specifically, two types of material were selected, including fabric (i.e., Nonwoven fabric) and flexible elastomer (i.e., PDMS), to simulate our daily encountered soft surfaces. The nonwoven fabric utilized in our experiment was 0.30 mm in thickness, and the PDMS used in our experiment was 0.10 mm in thickness.

Both *Accuracy* and *Reaction Time* were measured. The sensation of three types of buttons, namely the linear button, the clicky button, and the self-lock button, was reported by the participants according to their perceived sensation after the haptic rendering. The accuracy is based on whether they recognized the correct type of button. The trigger was enabled with the force sensor that continuously monitored the pressure. If the pressure exceeded the set threshold due to finger pressing, haptic rendering was triggered and timing started. The users pressed a button on the other hand to stop the timer when they recognized the haptic pattern.

5.2 Participants

Twelve (12) participants (5 females, avg. age = 24.75) were recruited randomly from a local university for the study. Each participant was fully informed about the experiment's context and procedures. The sequence of tests was randomly distributed.

5.3 Deployment Methods

The study was conducted in a quiet laboratory for two consecutive days. A laptop computer ran the experimental software, which controlled HapTag (Figure 9a). The participants were informed that they could stop the study at any time without giving any reasons (no participant terminated the study). The three interaction gestures were counterbalanced according to the Latin Square design and each set of tests (for one tactile response, one surface material, and one interaction gesture) was carried out 9 times. In total, 9 times * 3 tactile responses * 2 surface materials * 3 interaction gestures = 162 trials were tested on one participant. Before the formal user study,

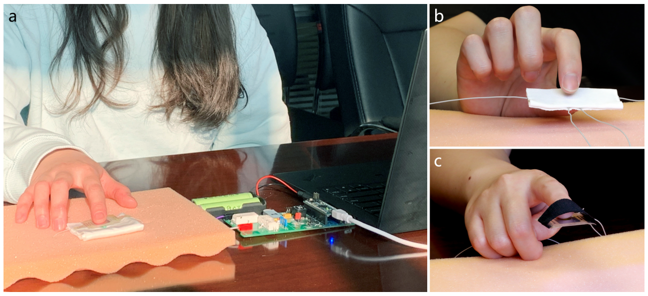

Figure 9: Experiment that evaluated HapTag. (a) The process of user testing; (b) pinch gestures; (c) In-air gestures.

participants firstly received a training section, where they were shown the three stimuli with each pattern 10 times repetitively in order.

5.4 Results

Based on our testings, we analyzed the result of participants' accuracy in recognizing the tactile responses and reaction time to respond on average to evaluate the feasibility and identifiability of our designed tactile responses and further, HapTag.

5.4.1 Accuracy. We conducted repeated measures ANOVA and Bonferroni corrected paired t-tests for pair-wise comparisons to compare the effects of the three IVs: the tactile responses, the surface materials, and the interaction gestures on the accuracy of recognizing the type of button. The repeated measures ANOVA yielded no significant effect on either Surface Material, Interaction Gestures, or Tactile Responses (all $p > 0.05$). Meanwhile, We found no statistically significant correlations between these three IVs ($p > 0.05$), neither of each of the three pairs of the listed two IVs (all $p > 0.05$). To better understand the effects of the above IVs, we plotted out the confusion matrix of accuracy at each haptic gesture, surface material, and tactile response, as shown in Figure 10.

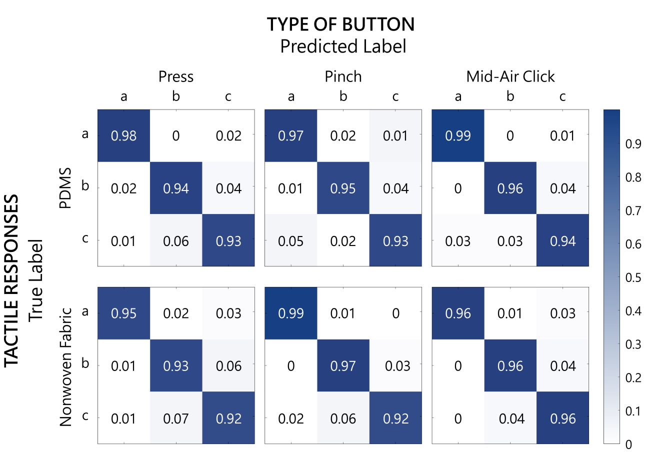

Figure 10: Confusion matrix of recognition results across the tactile responses, the surface materials and the interaction gestures. a: linear button; b: clikcy button; c: self-lock button.

The mean accuracy of recognized type of button is shown in Figure 11. As suggested by the figure, the mean accuracy varies in each set of tests. The highest mean accuracy is exhibited in the combination of PDMS, pinching gesture, and the tactile response simulating the haptic sensation of linear button, which is 100%. the lowest mean accuracy is shown in the combination of PDMS, pressing gesture, and the tactile response simulating the haptic sensation of both the linear button and the self-lock button, which is 90.7%. Besides, the tactile response that simulates different buttons varies, such as linear button(97.33 ± 1.63%), clikcy button (95.17 ± 1.47%), and the self-lock button (93.33 ± 1.50%). While for the integration materials, PDMS provides better accuracy (95.44 ± 2.19%) compared to nonwoven fabric (95.11 ± 2.37%). For the interaction gestures, mid-air pressing shows the highest accuracy (96.17 ± 1.60%), which is followed by pinching (95.50 ± 2.66%) and pressing (94.17 ± 2.14%).

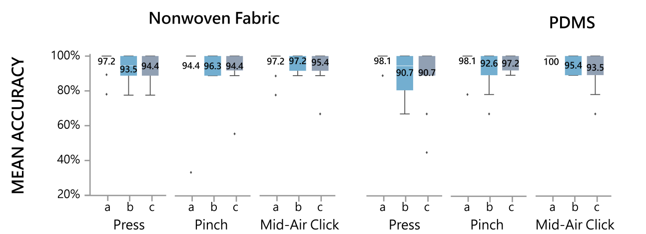

Figure 11: Mean Accuracy of Recognized Type of Button. a: linear button; b: clicky button; c: self-lock button.

5.4.2 Response Time. A repeated measures ANOVA and Bonferroni corrected paired t-tests for pair-wise comparisons were conducted to compare the significant effects of the three IVs: the tactile responses, the surface materials, and the interaction gestures on the continuous dependent variable, in our case, response time. The repeated measures ANOVA yielded a significant effect on Tactile Responses ($F(2, 22) = 10.32, p < 0.05$), but no significant effect was found on the other two factors. Meanwhile, no statistically significant three-way interaction of these three IVs ($p > 0.05$) was found. Also, there were no statistically significant differences in the simple two-way interactions for each pair of two IVs (all $p > 0.05$).

To better understand the effects of the IVs, we plotted out the mean response time at each haptic gesture, surface material, and tactile response, as shown in Figure 12.

For the average response time, the linear button shows the lowest response time (545.67 ± 22.96ms) compared to clikcy button (698.00 ± 119.08ms) and self-lock button (639.5 ± 55.17ms). For the integration material, nonwoven fabric shows a lower response time (621.33 ± 76.07ms) when compared to PDMS (636.56 ± 118.22ms). The response time for interaction gestures also varies: pressing (631.17 ± 93.21ms), pinching (592.67 ± 33.00ms) and mid-air pressing (659.33 ± 139.49ms)

5.5 Discussion

As shown in the results, the overall performance indicates that HapTag is able to generate haptic feedback that could be accurately recognized by participants. Based on the results, we found that the tactile response that simulated linear button was the most well-recognized pattern, compared to the pattern simulating clicky button and self-lock button. Compared to nonwoven fabric, HapTag integrated into PDMS also led to higher recognition accuracy. The mid-air pressing is the interaction gesture that could be recognized most accurately simulated by HapTag.

The results indicated the three tactile responses have no significant difference regarding the recognition rate, while the participants took a shorter time to perceive the linear button. This is probably due to the participants having some difficult time distinguishing between the clicky button and the self-lock button, but eventually, they got the right answer. This suggests that though the tactile feedback of the two buttons can be clearly rendered and distinguished, they shall be further improved to add more distinguishable signatures.

The experiment results suggest the current selection of surface materials does not affect the recognition rate or response time. Further investigation is needed to figure out the possible effects of other surface materials for constructing design suggestions.

The statistical differences between tactile responses, integration materials and interaction gestures were trivial, which was qualitatively supported by the following three-way repeated measures ANOVA test. The three-way repeated measures ANOVA test results indicate that there is no significant effect of each of the IVs on both the response accuracy and the response time. While according to the calculated confusion matrix, the accuracy of all sets of the experiment is higher than 92%. Such a high accuracy of users' responses suggests that our design is robust in our experimental environment to be easily adaptive to user habits and engagements and also susceptible to being applied in different sets of surface materials, interaction gestures, and tactile responses.

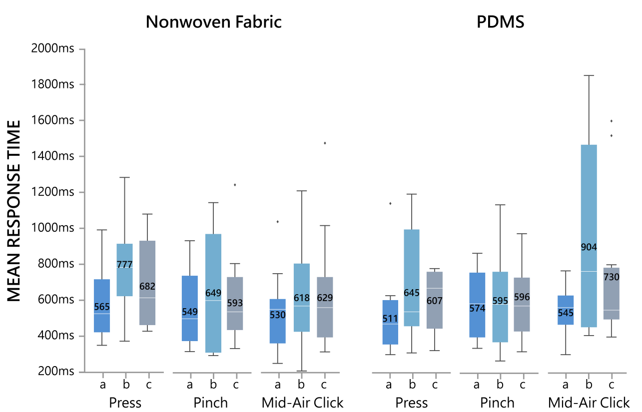

Figure 12: Mean Response Time. a: linear button; b: clicky button; c: self-lock button.

6 DISCUSSION

With the development of HapTag, we first adopt the emerging HASEL actuators for haptic interfaces that produce push-button haptic feedback. We demonstrated the feasibility and reliability of using HapTag to support push button tactile rendering on daily soft surfaces. This helps extend the vision of anywhere-touch interactions. The design choice of the material and customized structure design was critical in building a HapTag. Compared with previous solutions that only deliver vibrotactile feedback, HapTag took advantage of being able to generate stronger and larger output force and displacement, respectively. We showed that such capabilities of HapTag enabled us to explore a rich set of tactile response profiles to simulate button-click feelings.

6.1 Application

HapTag can be used in a rich set of scenarios, to provide users with sensational haptic feedback while they interact with "button" on regular soft surfaces. Here we list several examples, to indicate how possible HapTag can be implanted on everyday surfaces to upgrade the interactions via adopting various haptic feedback. For instance, HapTag can be stitched to sleeves or cuffs, to allow users to pinch the button with two fingers to answer a phone call (Figure 1b). In this way, it turns regular clothes into an interactive interface with control element - buttons. Also, taking the benefits of the thin and flexible formfactor of HapTag, this formfactor allows designers to maintain the cloth's fashionable features and original texture of fabrics. Similar ideas were composed and demonstrated with Figure 1c, where a smartwatch wristband made of rubber materials merged with a HapTag. Users can press the button to give UI commands to the watch. This setup enables physical button-like haptic experiences without affecting the original functions of the watch.

Other potential uses of Haptag include integrating, attaching, or embedding it to a bottle protective case, an inflated bag, the armrest of a sofa, the shoulder strap of a backpack, and a finger cot, and introducing button click sensations to pressing on daily objects and mid-air click interactions, respectively (Figure 13). Additionally, the active actuation of HapTag can be used as a tangible indicator. For example, with the bottle protective case embedded with HapTag, the bottle can inform users of an incoming meeting by actively actuating HapTag, and users confirm the message by pressing it back. HapTag is also able to turn a regular inflated bag into a game controller, with the enriched sensations of the button press. Mid-air interactions are common for VR/AR applications, but it is critical to have haptic feedback to enrich user experiences. HapTag provides a promising approach to building thin and flexible wearable haptic devices, which are mostly bulky and rigid at the current stage.

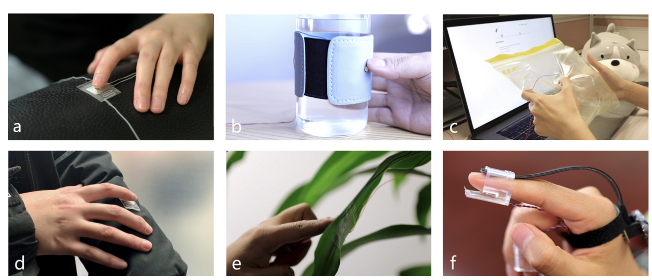

Figure 13: Proposed scenarios that could be benefited by HapTag. (a) HapTag integrated on sofa; (b) HapTag embedded in a mug cover; (c) HapTag integrated on flexible film bags; (d) HapTag embedded in the sleeve; (e) HapTag attached to the leaves; (f) Mid-air interactions with HapTag.

6.2 Limitation and Future Work

This work was the first step in exploring deployable haptic tags or patches, that can be used for daily soft surfaces. We found it is important to include the input sensing on HapTag to design the actuating mechanism that is responsive to user actions. For instance, it is important to be able to identify a user's touch and pressure level, and use that information to activate the actuation of HapTag. The challenge here is that the integrated pressure sensor has to be responsive to any changes on soft surfaces upon users' contact, while the actuation of HapTag introduced additional force that alters the reading of the pressure sensor instantly. In our case, the pressure sensor was used mainly as a trigger mechanism, and we assumed that users did not do slow motions when pressing on the surfaces, thus real-time analysis of the pressure sensor readings was not necessary at the current step. However, it would require further evaluation if the finer sensing-actuating relationship is required.

Force rendering is an important feature in this work. We have explained that to create more realistic button click feelings, it is critical to generate proper force-displacement characteristics. In this work, we used only three types of physical buttons as references to create the profiles. The profiles can be more expressive to adopt HapTag in a richer set of applications. In the next step, we will explore more examples, and refine the methods to control the force rendering to vary the output force based on displacement information.

Another important aspect to consider is the compatibility between HapTag and other surface materials. First, current implementations temporally attached or inserted a HapTag to the surfaces for demonstration and evaluation purposes. A permanent attachment method shall be figured out for supporting its practical deployment. Second, whether attaching a HapTag onto different materials would affect its generated haptic feedback would be a further explorable question, worthy to be studied in future work. Investigating its adaptation to different environments works as important guidance for a HapTag's applicable design.

On customizability, in addition to adjusting the input voltage and frequency, the size and the shape of the cover layer can vary to resemble different shapes of buttons, such as those with rectangles. Multiple HapTag buttons can be collocated or stacked, as shown in [1, 16].

Besides, different people also showed different average accuracy and response time, which may due to people's diverse threshold of tactile sensation. According to the previous study[14], the tactile threshold of the different parts of the skin also different, which suggests that a standard benchmark should be set to ensure the customized design according to people's diversity in haptic sensitivity.

As for the fabrication, we have tried but did not choose materials such as PVDF or P (VDF-Trfe-Ctfe) with higher dielectric constants. Because their softness is relatively hard, the manufacturing process is more complicated, and the cost will be much higher than the common TPU materials in daily life. HapTag actuators maintained proper performances in the user experiment, where each HapTag used up to 6 hours and rendered patterns about 1300 times. However, further study is needed to formally evaluate durability and safety.

7 CONCLUSION

HapTag is a thin and compact device that can render various haptic outputs to simulate push buttons. It can be attached or integrated into surrounding soft surfaces for daily touch interactions. HapTag is built under the principle of HASEL, while modified in material and structure to provide pressure sensing input, and force and out-of-plane displacement output. Three different types of push button tactile responses were composed, based on the tuning of force-displacement curves, which were tested distinguishable in our user study. The prototype of HapTag was visioned to fit into different soft surface materials, and we demonstrated how applicable HapTag can be embedded in daily soft surfaces to enrich button based interactions in abundant scenarios.

ACKNOWLEDGMENTS

This work was supported by the National Natural Science Foundation of China under Grant No. 61972387. Our sincere thanks to all the participants in the experiment.

REFERENCES

[1] Eric Acome, Shane K Mitchell, TG Morrissey, MB Emmett, Claire Benjamin, Madeline King, Miles Radakovitz, and Christoph Keplinger. 2018. Hydraulically amplified self-healing electrostatic actuators with muscle-like performance. *Science* 359, 6371 (2018), 61–65.

[2] Asma Akther, Jasmine O Castro, Seyed Ali Mousavi Shaegh, Amgad R Rezk, and Leslie Y Yeo. 2019. Miniaturised acoustofluidic tactile haptic actuator. *Soft matter* 15, 20 (2019), 4146–4152.

[3] David S. Alles. 1970. Information Transmission by Phantom Sensations. *IEEE Transactions on Man-Machine Systems* 11, 1 (1970), 85–91. https://doi.org/10.1109/TMMS.1970.299967

[4] Cagatay Basdogan, Frederic Giraud, Vincent Levesque, and Seungmoon Choi. 2020. A review of surface haptics: enabling tactile effects on touch surfaces. *IEEE transactions on haptics* 13, 3 (2020), 450–470.

[5] Olivier Bau, Ivan Poupyrev, Ali Israr, and Chris Harrison. 2010. *TeslaTouch: Electrovibration for Touch Surfaces.* Association for Computing Machinery, New York, NY, USA, 283–292. https://doi.org/10.1145/1866029.1866074

[6] Sean Follmer, Daniel Leithinger, Alex Olwal, Nadia Cheng, and Hiroshi Ishii. 2012. Jamming User Interfaces: Programmable Particle Stiffness and Sensing for Malleable and Shape-Changing Devices. In *Proceedings of the 25th Annual ACM Symposium on User Interface Software and Technology* (Cambridge, Massachusetts, USA) *(UIST '12)*. Association for Computing Machinery, New York, NY, USA, 519–528. https://doi.org/10.1145/2380116.2380181

[7] Sean Follmer, Daniel Leithinger, Alex Olwal, Akimitsu Hogge, and Hiroshi Ishii. 2013. InFORM: Dynamic Physical Affordances and Constraints through Shape and Object Actuation. In *Proceedings of the 26th Annual ACM Symposium on User Interface Software and Technology* (St. Andrews, Scotland, United Kingdom) *(UIST '13)*. Association for Computing Machinery, New York, NY, USA, 417–426. https://doi.org/10.1145/2501988.2502032

[8] Christian Frisson, Julien Decaudin, Thomas Pietrzak, Alexander Ng, Pauline Poncet, Fabrice Casset, Antoine Latour, and Stephen A. Brewster. 2017. Designing Vibrotactile Widgets with Printed Actuators and Sensors. In *Adjunct Publication of the 30th Annual ACM Symposium on User Interface Software and Technology* (Québec City, QC, Canada) *(UIST '17)*. Association for Computing Machinery, New York, NY, USA, 11–13. https://doi.org/10.1145/3131785.3131800

[9] S Grimnes. 1983. Electrovibration, cutaneous sensation of microampere current. *Acta Physiologica Scandinavica* 118, 1 (1983), 19–25.

[10] Daniel Groeger, Martin Feick, Anusha Withana, and Jürgen Steimle. 2019. Tactlets: Adding Tactile Feedback to 3D Objects Using Custom Printed Controls. In *Proceedings of the 32nd Annual ACM Symposium on User Interface Software and Technology* (New Orleans, LA, USA) *(UIST '19)*. Association for Computing Machinery, New York, NY, USA, 923–936. https://doi.org/10.1145/3332165.3347937

[11] Juan J Huaroto, Victor Ticllacuri, Etsel Suarez, Robert Ccorahua, and Emir A Vela. 2019. A Soft Pneumatic Haptic Actuator Mechanically Programmed for Providing Mechanotactile Feedback. *MRS Advances* 4, 19 (2019), 1131–1136.

[12] Apple Inc. 2021. *Human Interface Guidelines: Haptics.* Retrieved September 6, 2021 from https://developer.apple.com/design/human-interface-guidelines/ios/user-interaction/haptics/

[13] Yvonne Jansen, Thorsten Karrer, and Jan Borchers. 2010. MudPad: Tactile Feedback and Haptic Texture Overlay for Touch Surfaces. In *ACM International Conference on Interactive Tabletops and Surfaces* (Saarbrücken, Germany)

(ITS '10). Association for Computing Machinery, New York, NY, USA, 11–14. https://doi.org/10.1145/1936652.1936655

[14] Lynette A Jones and Susan J Lederman. 2006. *Human hand function.* Oxford university press.

[15] Yei Hwan Jung, Jae-Hwan Kim, and John A Rogers. 2020. Skin-Integrated Vibrohaptic Interfaces for Virtual and Augmented Reality. *Advanced Functional Materials* (2020), 2008805.

[16] Edouard Leroy, Ronan Hinchet, and Herbert Shea. 2020. Multimode hydraulically amplified electrostatic actuators for wearable haptics. *Advanced Materials* 32, 36 (2020), 2002564.

[17] Yi-Chi Liao, Sunjun Kim, Byungjoo Lee, and Antti Oulasvirta. 2020. *Button Simulation and Design via FDVV Models.* Association for Computing Machinery, New York, NY, USA, 1–14. https://doi.org/10.1145/3313831.3376262

[18] Alex Mazursky, Shan-Yuan Teng, Romain Nith, and Pedro Lopes. 2021. *MagnetIO: Passive yet Interactive Soft Haptic Patches Anywhere.* Association for Computing Machinery, New York, NY, USA. https://doi.org/10.1145/3411764.3445543

[19] Shane K Mitchell, Trent Martin, and Christoph Keplinger. [n.d.]. A Pocket-Sized Ten-Channel High Voltage Power Supply for Soft Electrostatic Actuators. *Advanced Materials Technologies* ([n. d.]), 2101469.

[20] Seongcheol Mun, Sungryul Yun, Saekwang Nam, Seung Koo Park, Suntak Park, Bong Je Park, Jeong Mook Lim, and Ki-Uk Kyung. 2018. Electro-active polymer based soft tactile interface for wearable devices. *IEEE transactions on haptics* 11, 1 (2018), 15–21.

[21] Mark Nagurka and Richard Marklin. 2005. Measurement of stiffness and damping characteristics of computer keyboard keys. (2005).

[22] T. Nara, M. Takasaki, T. Maeda, T. Higuchi, S. Ando, and S. Tachi. 2001. Surface acoustic wave tactile display. *IEEE Computer Graphics and Applications* 21, 6 (2001), 56–63. https://doi.org/10.1109/38.963461

[23] Alex Olwal, Jon Moeller, Greg Priest-Dorman, Thad Starner, and Ben Carroll. 2018. I/O Braid: Scalable Touch-Sensitive Lighted Cords Using Spiraling, Repeating Sensing Textiles and Fiber Optics. In *Proceedings of the 31st Annual ACM Symposium on User Interface Software and Technology* (Berlin, Germany) *(UIST '18)*. Association for Computing Machinery, New York, NY, USA, 485–497. https://doi.org/10.1145/3242587.3242638

[24] Antti Oulasvirta, Sunjun Kim, and Byungjoo Lee. 2018. *Neuromechanics of a Button Press.* Association for Computing Machinery, New York, NY, USA, 1–13. https://doi.org/10.1145/3173574.3174082

[25] Ailish O'Halloran, Fergal O'malley, and Peter McHugh. 2008. A review on dielectric elastomer actuators, technology, applications, and challenges. *Journal of Applied Physics* 104, 7 (2008), 9.

[26] Chaeyong Park, Jinhyuk Yoon, Seungjae Oh, and Seungmoon Choi. 2020. Augmenting Physical Buttons with Vibrotactile Feedback for Programmable Feels. In *Proceedings of the 33rd Annual ACM Symposium on User Interface Software and Technology* (Virtual Event, USA) *(UIST '20)*. Association for Computing Machinery, New York, NY, USA, 924–937. https://doi.org/10.1145/3379337.3415837

[27] Gunhyuk Park and Seungmoon Choi. 2018. *Tactile Information Transmission by 2D Stationary Phantom Sensations.* Association for Computing Machinery, New York, NY, USA, 1–12. https://doi.org/10.1145/3173574.3173832

[28] Ron Pelrine, Roy Kornbluh, Qibing Pei, and Jose Joseph. 2000. High-speed electrically actuated elastomers with strain greater than 100%. *Science* 287, 5454 (2000), 836–839.

[29] Ron Pelrine, Qibing Pei, and Roy Kornbluh. 2018. Dielectric elastomers: past, present, and potential future. In *Electroactive Polymer Actuators and Devices (EAPAD) XX*, Vol. 10594. International Society for Optics and Photonics, 1059406.

[30] Ivan Poupyrev, Nan-Wei Gong, Shiho Fukuhara, Mustafa Emre Karagozler, Carsten Schwesig, and Karen E. Robinson. 2016. Project Jacquard: Interactive Digital Textiles at Scale. In *Proceedings of the 2016 CHI Conference on Human Factors in Computing Systems* (San Jose, California, USA) *(CHI '16)*. Association for Computing Machinery, New York, NY, USA, 4216–4227. https://doi.org/10.1145/2858036.2858176

[31] Robert G Radwin and Barry A Ruffalo. 1999. Computer key switch force-displacement characteristics and short-term effects on localized fatigue. *Ergonomics* 42, 1 (1999), 160–170.

[32] Jussi Rantala, Katri Salminen, Roope Raisamo, and Veikko Surakka. 2013. Touch Gestures in Communicating Emotional Intention via Vibrotactile Stimulation. *Int. J. Hum.-Comput. Stud.* 71, 6 (June 2013), 679–690. https://doi.org/10.1016/j.ijhcs.2013.02.004

[33] Munehiko Sato, Ivan Poupyrev, and Chris Harrison. 2012. *Touché: Enhancing Touch Interaction on Humans, Screens, Liquids, and Everyday Objects.* Association for Computing Machinery, New York, NY, USA, 483–492. https://doi.org/10.1145/2207676.2207743

[34] Samuel Schlatter, Patrin Illenberger, and Samuel Rosset. 2018. Peta-pico-Voltron: An open-source high voltage power supply. *HardwareX* 4 (2018), e00039.

[35] Y. Sekiguchi, K. Hirota, and M. Hirose. 2005. The design and implementation of ubiquitous haptic device. In *First Joint Eurohaptics Conference and Symposium on Haptic Interfaces for Virtual Environment and Teleoperator Systems. World Haptics Conference.* 527–528. https://doi.org/10.1109/WHC.2005.128

[36] Tanay Singhal and Oliver Schneider. 2021. *Juicy Haptic Design: Vibrotactile Embellishments Can Improve Player Experience in Games.* Association for Computing Machinery, New York, NY, USA. https://doi.org/10.1145/3411764.3445463

[37] Alexa F. Siu, Eric J. Gonzalez, Shenli Yuan, Jason B. Ginsberg, and Sean Follmer. 2018. *ShapeShift: 2D Spatial Manipulation and Self-Actuation of Tabletop Shape Displays for Tangible and Haptic Interaction.* Association for Computing Machinery, New York, NY, USA, 1–13. https://doi.org/10.1145/3173574.3173865

[38] Harshal A Sonar, Aaron P Gerratt, Stéphanie P Lacour, and Jamie Paik. 2020. Closed-loop haptic feedback control using a self-sensing soft pneumatic actuator skin. *Soft robotics* 7, 1 (2020), 22–29.

[39] Robert M. Strong and Donald E. Troxel. 1970. An Electrotactile Display. *IEEE Transactions on Man-Machine Systems* 11, 1 (1970), 72–79. https://doi.org/10.1109/TMMS.1970.299965

[40] Linzhi Tang and Nae Yoon Lee. 2010. A facile route for irreversible bonding of plastic-PDMS hybrid microdevices at room temperature. *Lab on a Chip* 10, 10 (2010), 1274–1280.

[41] Quang Van Duong, Vinh Phu Nguyen, Fabrice Domingues Dos Santos, and Seung Tae Choi. 2019. Localized fretting-vibrotactile sensations for large-area displays. *ACS applied materials & interfaces* 11, 36 (2019), 33292–33301.

[42] Siarhei Vishniakou, Brian W Lewis, Xiaofan Niu, Alireza Kargar, Ke Sun, Michael Kalajian, Namseok Park, Muchuan Yang, Yi Jing, Paul Brochu, et al. 2013. Tactile feedback display with spatial and temporal resolutions. *Scientific reports* 3, 1 (2013), 1–7.

[43] Xingrui Wang, Shane K Mitchell, Ellen H Rumley, Philipp Rothemund, and Christoph Keplinger. 2020. High-strain peano-HASEL actuators. *Advanced Functional Materials* 30, 7 (2020), 1908821.

[44] Michael Wessely, Ticha Sethapakdi, Carlos Castillo, Jackson C. Snowden, Ollie Hanton, Isabel P. S. Qamar, Mike Fraser, Anne Roudaut, and Stefanie Mueller. 2020. *Sprayable User Interfaces: Prototyping Large-Scale Interactive Surfaces with Sensors and Displays.* Association for Computing Machinery, New York, NY, USA, 1–12. https://doi.org/10.1145/3313831.3376249

[45] Michael Wiertlewski, José Lozada, and Vincent Hayward. 2011. The Spatial Spectrum of Tangential Skin Displacement Can Encode Tactual Texture. *IEEE Transactions on Robotics* 27, 3 (2011), 461–472. https://doi.org/10.1109/TRO.2011.2132830

[46] Laura Winfield, John Glassmire, J. Edward Colgate, and Michael Peshkin. 2007. T-PaD: Tactile Pattern Display through Variable Friction Reduction. In *Second Joint EuroHaptics Conference and Symposium on Haptic Interfaces for Virtual Environment and Teleoperator Systems (WHC'07).* 421–426. https://doi.org/10.1109/WHC.2007.105

[47] Tae-Heon Yang, Hyungki Son, Sangkyu Byeon, Hyunjae Gil, Inwook Hwang, Gwanghyun Jo, Seungmoon Choi, Sang-Youn Kim, and Jin Ryong Kim. 2021. Magnetorheological Fluid Haptic Shoes for Walking in VR. *IEEE Transactions on Haptics* 14, 1 (2021), 83–94. https://doi.org/10.1109/TOH.2020.3017099

[48] Yongjae Yoo, Taekbeom Yoo, Jihyun Kong, and Seungmoon Choi. 2015. Emotional responses of tactile icons: Effects of amplitude, frequency, duration, and envelope. In *2015 IEEE World Haptics Conference (WHC).* 235–240. https://doi.org/10.1109/WHC.2015.7177719

[49] Sang Ho Yoon, Siyuan Ma, Woo Suk Lee, Shantanu Thakurdesai, Di Sun, Flávio P. Ribeiro, and James D. Holbery. 2019. HapSense: A Soft Haptic I/O Device with Uninterrupted Dual Functionalities of Force Sensing and Vibrotactile Actuation. In *Proceedings of the 32nd Annual ACM Symposium on User Interface Software and Technology* (New Orleans, LA, USA) *(UIST '19)*. Association for Computing Machinery, New York, NY, USA, 949–961. https://doi.org/10.1145/3332165.3347888

[50] Sang Ho Yoon, Siyuan Ma, Woo Suk Lee, Shantanu Thakurdesai, Di Sun, Flávio P Ribeiro, and James D Holbery. 2019. HapSense: A soft haptic I/O device with uninterrupted dual functionalities of force sensing and vibrotactile actuation. In *Proceedings of the 32nd Annual ACM Symposium on User Interface Software and Technology.* 949–961.

[51] Xinge Yu, Zhaoqian Xie, Yang Yu, Jungyup Lee, Abraham Vazquez-Guardado, Haiwen Luan, Jasper Ruban, Xin Ning, Aadeel Akhtar, Dengfeng Li, et al. 2019. Skin-integrated wireless haptic interfaces for virtual and augmented reality. *Nature* 575, 7783 (2019), 473–479.

[52] Yichen Zhai, Zhijian Wang, Kye-Si Kwon, Shengqiang Cai, Darren J Lipomi, and Tse Nga Ng. 2021. Printing Multi-Material Organic Haptic Actuators. *Advanced Materials* 33, 19 (2021), 2002541.

[53] Yang Zhang and Chris Harrison. 2018. *Pulp Nonfiction: Low-Cost Touch Tracking for Paper.* Association for Computing Machinery, New York, NY, USA, 1–11. https://doi.org/10.1145/3173574.3173691

[54] Yang Zhang, Chouchang (Jack) Yang, Scott E. Hudson, Chris Harrison, and Alanson Sample. 2018. *Wall++: Room-Scale Interactive and Context-Aware Sensing.* Association for Computing Machinery, New York, NY, USA, 1–15. https://doi.org/10.1145/3173574.3173847